http://dx.doi.org/10.1590/0104-1428.2376

Simulation of temperature effect on the structure control of polystyrene obtained by atom-transfer radical polymerization

Roniérik Pioli Vieira[1,2]* and Liliane Maria Ferrareso Lona[2]

[1]Instituto Federal de Educação, Ciência e Tecnologia do Sul de Minas Gerais – IFSULDEMINAS, Pouso Alegre, MG, Brazil

[2]Laboratory of Analysis, Simulations and Synthesis of Chemical Processes, School of Chemical Engineering, Universidade Estadual de Campinas – UNICAMP, Campinas, SP, Brazil

**ronierik@ymail.com*

Abstract

This paper uses a new kinetic modeling and simulations to analyse the effect of temperature on the polystyrene properties obtained by atom-transfer radical polymerization (ATRP). Differently from what has been traditionaly published in ATRP modeling works, it was considered "break" reactions in the mechanism aiming to reproduce the process at high temperatures. Results suggest that there is an upper limit temperature (130 °C), above which the polymer architecture loses the control. In addition, for the system considered in this work, the optimum operating temperature was 100 °C, because at this temperature polymer with very low polydispersity index is obtained, at considerable fast polymerization rate. Therefore, this present paper provides not only a tool to study ATRP processes by simulations, but also a tool for analysis and optimization, being a basis for future works dealing with this monomer and process.

Keywords: *ATRP, kinetic modeling, simulation, radical polymerization.*

1. Introduction

Atom-transfer radical polymerization (ATRP) is a powerful technique for controlled synthesis of polymers that provides several macromolecular architectures: polymers with narrow molecular weight distribution[1], block copolymers[2,3], random or gradient[4] and functionalized polymers[5-9]. ATRP has a great interest in the academic and industrial field because it can be used for various monomers, can be conducted in mild temperatures, and it is very resistant to impurities[10].

ATRP has been used industrially since 2005 with commercial products being manufactured in the US, Japan, and Europe. Some fundamental processes based on low catalyst, such as ARGET and ICAR ATRP, should soon be introduced to commercial sacales, but further scale-up will require synergistic input from process engineering, converting batch systems to continuous processes, transport phenomena, and accounting for complex stabilities such as temperature[10,11].

Profound mechanistic understanding is needed not only for optimization of the ATRP process but also to expand the range of polymerizable monomers, reduce the amount of catalyst, and allow synthesis of better defined polymers[11,12], which are related mostly with temperature. This is one of the most important variables in controlled polymerization systems, since it has a considerable influence on the polymerization rate and polymer properties. High temperatures accelerates the process, but provides high dispersity values which is not desirable.

An analysis of temperature effect should provide directions for optimizations in ATRP, and also set a temperature limit for a particular system. This limit should be a value that keep track of the formed polymer structure. As far as is known, modelling works available in literature did not address effects of temperature directly on the molecular weight and dispersities[12,13]. As a result, the polymerization control limit was also not explored properly[14]. Based on these observations, there is the need to demonstrate the effect of this variable on the polymer properties and the polymerization rate so that the readers may apply to other systems.

The aim of this paper is to analyze the effect of temperature on the polymer properties and polymerization rate in ATRP by providing a limit for the styrene polymerization using CuBr/PMDETA as catalyst system. Therefore, this present research will be able to be used in future process optimization researches, which must have a value such that the polymerization control is not lost.

2. Kinetic Modeling

Traditional researches on ATRP modeling have not been considered "break" reactions in the process such as chain transfer and terminations[13-19]. This current approach incorporates some reactions into the model aiming reproduce the sytem at high temperatures, which were usually considered in conventional polymerizations. This approach was validated in a previus research of our group[20,21], and the kinetic mechanism are shown in Equations 1-11.

SCIENTIFIC ARTICLE

- Initiation:

$$RX + C \xleftrightarrow{Keq} R^{\bullet} + XC \quad (1)$$

$$R^{\bullet} + M \xrightarrow{ki} P_1 \quad (2)$$

$$3M \xrightarrow{ktherm} 2R^{\bullet} \quad (3)$$

$$2M \xrightarrow{k\,\mathrm{dim}} D \quad (4)$$

- Propagation:

$$P_n X + C \xleftrightarrow{Keq} P_n^{\bullet} + XC \quad (5)$$

$$P_n^{\bullet} + M \xrightarrow{kp} P_{n+1}^{\bullet} \quad (6)$$

- Termination:

$$P_n^{\bullet} + P_m^{\bullet} \xrightarrow{ktc} P_{n+m} \quad (7)$$

$$P_n^{\bullet} + P_m^{\bullet} \xrightarrow{ktd} P_n + P_m \quad (8)$$

$$P_n^{\bullet} + R^{\bullet} \xrightarrow{ktc} P_n \quad (9)$$

- Chain transfer:

$$P_n^{\bullet} + M \xrightarrow{ktr,M} P_n + R^{\bullet} \quad (10)$$

$$P_n^{\bullet} + D \xrightarrow{ktr,D} P_n + P_1 \quad (11)$$

Equations 1 through 11 are the chemical mechanism considered to represent the ATRP procces in this present paper. In such equations there are the some reactions traditionally used to represent the system: initiation step (Equation 1 and 2), the chemical equilibrium involving the propagation and dormant species (Equation 5), propagation of polymer chains (Equation 6), termination by combination (Equation 7), termination by disproportionation (Equation 8) and chain transfer to monomer (Equation 10).

In addition to the reactions usually considered in ATRP, this paper proposed the inclusion of the following reactions: thermal initiation (Equation 3); dimerization reaction (Equation 4); termination caused by the reaction between the propagating species and a primary radical (Equation 9) and chain transfer to the dimer (Equation 11). The choice of these reactions was based on the conventional polymerizations in which these reactions are common at high temperatures. Such reactions have been considered in order to make the modeling more robust to represent the monomer conversion and the average properties at temperatures above 100 °C.

Kinetic model was developed based on the mechanism proposed in Equations 1-11. From this mechanism, we carried out a material balance in order to account for the variation of the following species: "living" polymers, "dead" polymers, "dormant" polymers, monomer, dimer and primary radicals. It was also used the well-known method of moments[18] to obtain average molecular weight (Mn and Mw) and polydispersity index (PDI).

A system of 12 ordinary differential equations was generate, which was solved numerically for all simulations of this present paper. The system consists of mass balance for monomer, primary radicals and dimer (Equations 12, 13 and 14), plus the moment equations (Equations 15 to 23): moments of order "zero", "one" and "two", referring to "living" polymer, "dead" polymer and "dormant" polymer. The kinetic modeling was simplified for a batch system without considerable volume variation.

$$\frac{d[M]}{dt} = -k_p[M]\mu_0 - 2k_{\mathrm{dim}}[M]^2 - k_{tr,M}[M]\mu_0 - k_i[R^{\bullet}][M] - k_{therm}[M]^3 \quad (12)$$

$$\frac{d[R^{\bullet}]}{dt} = -k_i[R^{\bullet}][M] + k_{therm}[M]^3 - k_{tp}[R^{\bullet}]\mu_0 \quad (13)$$

$$\frac{d[D]}{dt} = +2k_{\mathrm{dim}}[M]^2 - k_{tr,D}[D]\mu_0 \quad (14)$$

$$\frac{d\mu_0}{dt} = k_a\delta_0([C]_0 - [RX]_0 + \delta_0) - k_{da}\mu_0([RX]_0 - \delta_0) - k_{tc}\mu_0^2 - k_{td}\mu_0^2 - k_{tp}[R^{\bullet}]\mu_0 - k_{tr,M}[M]\mu_0 - k_{tr,D}[D]\mu_0 \quad (15)$$

$$\frac{d\delta_0}{dt} = k_{da}\mu_0([RX]_0 - \delta_0) - k_a\delta_0([C]_0 - [RX]_0 + \delta_0) \quad (16)$$

$$\frac{d\lambda_0}{dt} = \frac{1}{2}k_{tc}\mu_0^2 + k_{td}\mu_0^2 + k_{tp}[R^{\bullet}]\mu_0 + k_{tr,M}[M]\mu_0 + k_{tr,D}[D]\mu_0 \quad (17)$$

$$\frac{d\mu_1}{dt} = k_p\mu_0[M] + k_a\delta_1([C]_0 - [RX]_0 + \delta_0) - k_{da}\mu_1([RX]_0 - \delta_0) - k_{tc}\mu_0\mu_1 - k_{tc}\mu_0\mu_1 - k_{tp}[R^{\bullet}]\mu_1 - k_{tr,M}[M]\mu_1 - k_{tr,D}[D]\mu_1 \quad (18)$$

$$\frac{d\delta_1}{dt} = -k_a\delta_1([C]_0 - [RX]_0 + \delta_0) + k_{da}\mu_1([RX]_0 - \delta_0) \quad (19)$$

$$\frac{d\lambda_1}{dt} = k_{tc}\mu_0\mu_1 + k_{td}\mu_0\mu_1 + k_{tp}[R^{\bullet}]\mu_1 + k_{tr,M}[M]\mu_1 + k_{tr,D}[D]\mu_1 \quad (20)$$

$$\frac{d\mu_2}{dt} = k_p\mu_0[M] + k_a\delta_2([C]_0 - [RX]_0 + \delta_0) - k_{da}\mu_2([RX]_0 - \delta_0) - k_{tc}\mu_0\mu_2 - k_{td}\mu_0\mu_2 - k_{tp}[R^{\bullet}]\mu_2 - k_{tr,M}[M]\mu_2 - k_{tr,D}[D]\mu_2 \quad (21)$$

$$\frac{d\delta_2}{dt} = -k_a\delta_2([C]_0 - [RX]_0 + \delta_0) + k_{da}\mu_2([RX]_0 - \delta_0) \quad (22)$$

$$\frac{d\lambda_2}{dt} = k_{tc}\mu_0\mu_2 + k_{td}\mu_0\mu_2 + k_{tp}[R^\bullet]\mu_2 + k_{tr,M}[M]\mu_2 + k_{tr,D}[D]\mu_2 \quad (23)$$

In Equations 12 a 23, $[M]$ is the monomer concentration; $[R^\bullet]$ is the primary radicas concentration; $[D]$ is the dimer concentration; μ is the moment for the "living" polymers with orders 0, 1 and 2 as subscrites; δ is the moment for the "dormant" polymers with orders 0, 1 and 2 as subscrites; λ is the moment for the "living" polymers with orders 0, 1 and 2 as subscrites; k_p is the kinetic rate coefficient of propagation; k_i is the kinetic rate coefficient of initiation; k_{therm} is the kinetic rate coefficient of termal initiation; k_{dim} is the kinetic rate coefficient of dimerization; k_a is the kinetic rate coefficient of activation; k_{da} is the kinetic rate coefficient of polymeric chain deactivation; k_{tc} is the kinetic rate coefficient of termination by combination; k_{td} is the kinetic rate coefficient of despoportionation; k_{tp} is the kinetic rate coefficient of termination by the reaction with a primar radical; $k_{tr,M}$ is the kinetic rate coefficient of chain transfer to moomer; and $k_{tr,D}$ is the kinetic rate coefficient of chain transfer to dimer.

3. Resolution of the Equations System

For the ODE's system solution it was developed a computer program in Fortran code with the aid of LSODE subroutine developed by Hindmarsh[22]. This subroutine uses the Adams-Moulton method to solve initial value problems. This subroutine was chosen because it is very efficient to solve problems with high numerical stiffness, which is quite common in polymer engineering[19,23,24].

To obtain the number-average molecular weight, we used values of moments of order "zero" and "one" for each species, as defined by Equation 24[18].

$$\overline{Mn} = MW_M\left(\frac{\mu_1 + \lambda_1 + \delta_1}{\mu_0 + \lambda_0 + \delta_0}\right) \quad (24)$$

where $\overline{Mn}$ is the polymer number average molecular weight and *MWM* is the monomer molecular weight.

The polymer weight-average molecular weight took into account the moments of order "one" and "two" for each species, and was calculated by Equation 25.

$$\overline{Mw} = MW_M\left(\frac{\mu_2 + \lambda_2 + \delta_2}{\mu_1 + \lambda_1 + \delta_1}\right) \quad (25)$$

where $\overline{Mw}$ is the polymer weight average molecular weight.

After obtaining $\overline{Mn}$ and $\overline{Mw}$, the polymer polydispersity index (*PDI*) was obtained by Equation 26.

$$PDI = \frac{\overline{Mw}}{\overline{Mn}} \quad (26)$$

The program input data refer to the initial concentrations of monomer, catalyst, ligand, initiator and operating temperature. Table 1 provides the set of initial conditions used to solve the equations system.

As shown in Table 1, all population moments were assigned initial values equal to zero once the concentrations present in the process are negligible at time very close to zero. The system considered in this case study is the bulk styrene polymerization initiated by 1-phenylethyl bromide (1-PEBr), copper (I) bromide (CuBr) as catalyst and N,N,N',N",N"-pentamethyldiethyllenetriamine as ligand. This system was chosen due to the wide availability of kinetic data as function of temperature, in addition to the fact that it is a widely used system. The kinetic parameters were calculated as temperature functions according Arrhenius' expressions shown in Table 2.

Table 2 provides the expressions to analyze the influence of temperature on the ATRP process. In addition to Arrhenius' expression in Table 2, there is the traditional gel effect correlation proposed by Hui and Hamielec that affects the termination rate coefficient (k_t). This constant depends on the monomer conversion and the parameters A_1, A_2 and A_3 which in turn are related to the operating temperature.

4. Results and Discussions

Using the kinetic model of this paper, computer simulations were performed considering different operating temperatures in order to analyze the influence of this parameter on the product. Figure 1 illustrates the monomer conversion as a function of polymerization time, considering an isothermal

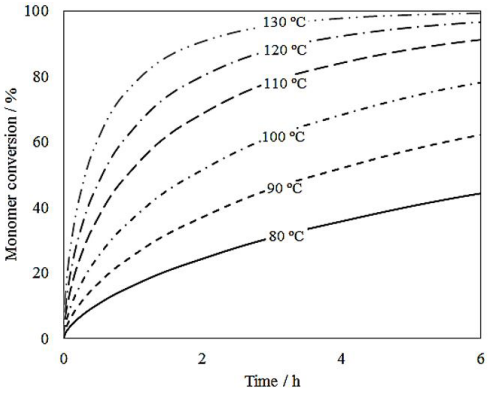

Figure 1. Styrene conversion simulation as a function of reaction time using 1-PEBr as initiator (0.087 mol L^{-1}), CuBr as catalyst (0.087 mol L^{-1}) and dH-bipy (0.174 mol L^{-1}) as binder six different temperatures (80, 90, 100, 110, 120 and 130 °C).

Table 1. Initial conditions used in the program for solving the differential model.

Parameter	Value (mol L^{-1})
$[M]_0$	8.7
$[RX]_0$	0.087
$[Mt^nY]_0$	0.087
$[L]_0$	0.174
$[D]_0$	0
$[R^*]_0$	0
All moments	0

Table 2. Expressions used to obtain the kinetic parameters for atom-transfer radical polymerization as functions of temperature.

Parameter	Expression	Reference
k_p	$4.226\times107\exp(-3910/T)$	Fu et al.[25]
k_i	$1.63\times10^6\exp(-12020/T)$	Fu et al.[25]
k_{therm}	$2.19\times10^5\exp(-13800/T)$	Fu et al.[25]
k_{dim}	$188.97\exp(-1947/T)$	Belincanta-Ximenes et al.[26]
k_a	$8.06\times10^5\exp(-4694,51/T)$	Seeliger and Matyjaszewski[27]
k_{da}	$3.860\times10^9\exp(-2245/T)$	Matyjaszewski[28]
k_{t0}	$3.820\times10^9\exp(-958/T)$	Fu et al.[25]
k_t	$k_{t0}\times\exp(-2\times(A_1X + A_2X^{[2]} + A_3X^{[3]}))$	Hui and Hamielec[29]
k_{tc}	$0.99k_t$	Fu et al.[25]
k_{td}	$0.01k_t$	Fu et al.[25]
$k_{t,p}$	10^9	Fischer and Paul[30]
$k_{tr,M}$	$2.310\times10^6\exp(-6377/T)$	Fu et al.[25]
$k_{tr,D}$	150	Fu et al.[25]
A_1	$2.57 - (5.05\times10^{-3}T)$	Hui and Hamielec[29]
A_2	$9.56 - (1.76\times10^{-2}T)$	Hui and Hamielec[29]
A_3	$-3.03 + (7.85\times10^{-3}T)$	Hui and Hamielec[29]

batch reactor operating at six different temperatures (80, 90, 100, 110, 120 and 130 °C).

An analysis of Figure 1 makes it clear that the increase of temperature is accompanied by an increase in the monomer conversion, confirming the polymerization rate is higher at higher temperatures. This result fits the step of the radical propagation as an irreversible reaction, whose rate coefficient is strongly dependent on temperature (high activation energy). Matyjaszewski[11] discusses this strong influence of temperature on the propagation rate coefficient (k_p). Moreover, the author also says that the activation step of dormant species (k_a) helps to increase the rate since the chemical equilibrium in Figure 2 tends to be shifted towards the formation of propagation radicals.

Figure 2 illustrates the equilibrium of polymer chains activation/deactivation in ATRP. The reagents are represented on the left side and the product on the right side. The energy associated with the products is greater than the energy associated with the reagents. There is an endothermic process for the activation of the polymer chains and thus increasing the system temperature favors the equilibrium constant displacement in this direction. As a result, there is a higher monomer conversion in Figure 1 because increasing the concentration of the propagating radicals caused an increase of reaction rate. Thus, considering optimize reaction time, it would be desirable to operate the system at the highest possible temperature in order to minimize the reactor size.

However, the temperature increase influences the chemical equilibrium in Figure 2, making the polymer properties be affected (Mn and IPD). The process tends, at high temperatures, to behave such as a conventional radical polymerization, that is, with a large amount of "living" radicals susceptible to termination and chain transfer. This is the great challenge of ATRP: be conducted at a temperature such that the concentration of "dormant" polymers is high and the concentration of "living" polymers is low. In this case, the most important issue is to meet the ideal temperature for a specific polymerization be conducted in the shortest possible time without losing the controlled polymerization characteristics.

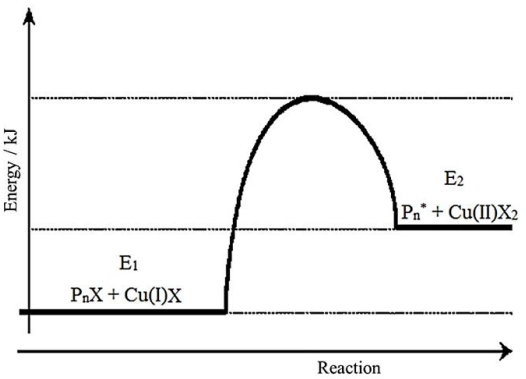

Figure 2. Typical energy profile for the equilibrium of activation/deactivation of the catalyst system in the ATRP processes, adapted from literature[10].

Figure 3 shows a linear evolution of Mn as a function of monomer conversion, featuring a controlled polymerization process. Comparing both profiles of molecular weights (Mn and Mw), it can be observed that there is a great difference between these values in low and high conversions. This occurs because, at the beginning of the ATRP process, the chemical equilibrium between the propagating radicals and the deactivator agent has not been established. As a result, a high concentration of primary radicals is generated, raising the probability of terminations at low monomer conversions.

In addition, there is also the same behavior that occurred at high monomer conversions, especially for the highest temperature analyzed (Figure 3c). This trend tends to be higher at elevated temperatures due to two factors: first because of the equilibrium displacement towards the formation of radicals in propagation (Figure 2) be favored. Second, due to the increase of kinetic rate coefficients of termination and chain transfer reactions, which led to the increase in the

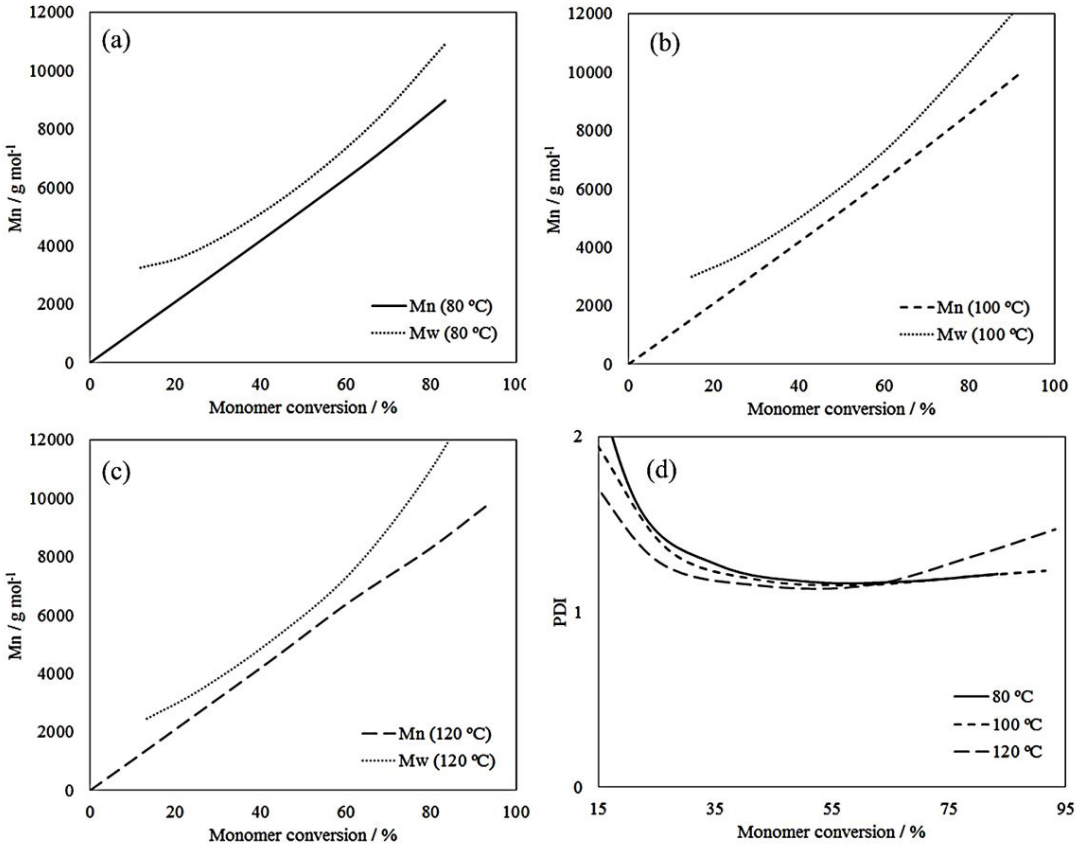

Figure 3. Simulations of number-average molecular weight (Mn) and weight-average molecular weight (Mw): (a) 80 °C; (b) 100 °C; (c) 120 °C and (d) comparison of the polydispersity ndexes in these temperatures.

concentration of "dead" polymers in the process (Figure 4 suggests there was a considerable increase in the concentration of "dead" polymer due to temperature increase).

It is important to highlight the polydispersities indexes that are shown in Figure 3d present the some differences in their profiles. For example, at low monomer conversions, high PDI values were obtained for all three simulations. To temperatures of 80 and 100 °C, the PDI values presented no significant differences in the simulated conversion range, remaining with low values. With this result, clearly, it would be ideal to work in a temperature around 100 °C, since it provides low values of PDI, and also this temperature increases the polymerization rate.

Moreover, for all simulated PDI profiles of Figure 3d, a coincident point was observed. This value is approximately 63% of monomer conversion. Finishing the polymerization in this range of conversion, the obtained polymers will have similar properties (Mn and PDI) for the three temperatures studied. This result suggests that it is possible to obtain polymers with a well-controlled structure at the highest temperature. The problem is related to the desired value of number-average molecular weight. In this case, the polymer obtained would show lower Mn values, around 6,500 g mol^{-1}, since the polymerization will be stoped at

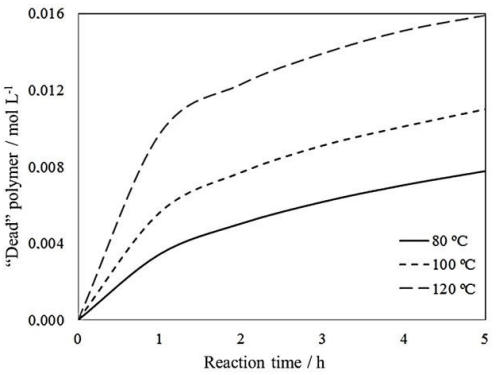

Figure 4. Simulation of the "dead" polymer concentration profile as a function of polymerization time at 80, 100 and 120 °C in styrene ATRP (8.7 mol L^{-1}) using 1-PEBr as initiator.

63% of conversion. Depending on the application, these characteristics would not be interesting.

Figure 5a and b illustrate a linear increase of Mn as a function of monomer conversion, differentiating from Figure 5c, wherein Mn presented deviations from linearity, characterizing as an uncontrolled polymerization. This result suggests that the temperature of 130 °C may be a limit of the

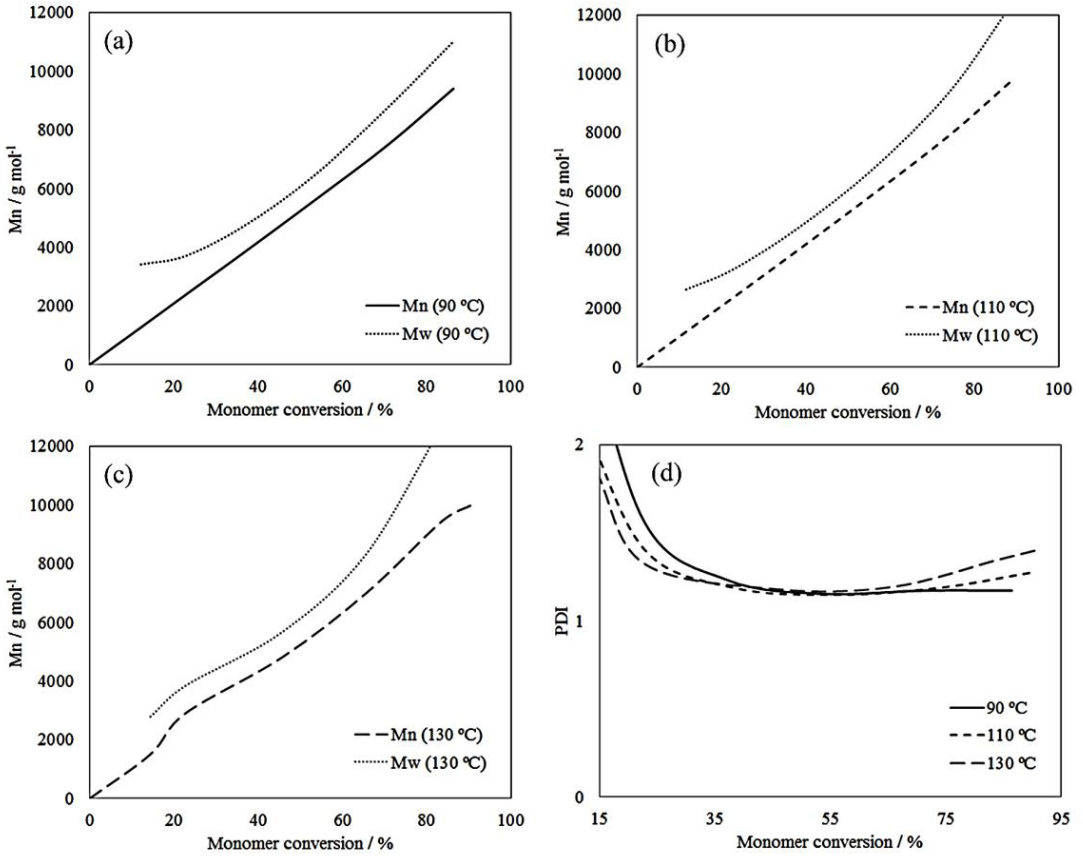

Figure 5. Simulations of number-average molecular weight (Mn) and weight-average molecular weight (Mw): (a) 90 °C; (b) 110 °C; (c) 130 °C and (d) comparison of the polydispersity ndexes in these temperatures.

system. At low temperatures (e.g. 90 °C), it is possible to obtain polymers with low PDI values in a large extension of the monomer conversion illustrated in Figure 5d. However, the polymerization rate is also very low. Thus, to obtain polymers with high molecular weight would be desirable to operate the reactor in a high residence time. Similarly to the result expressed in Figure 3d, for all temperature profiles, there is a conversion range (40 to 60%) that the PDI profiles are coincident, so it is possible to obtain similar polymer properties in this range. Comparing all PDI profiles of Figure 3 and 5 it can be seen that for the tested temperatures, 100 °C would be ideal, as they provide low PDI values at high monomer conversions. Moreover, such a reaction temperature provided a fast reaction rate without loss of controlled polymerization characteristics.

5. Conclusions

The main objective of this paper was to stablished a temperature limit for styrene ATRP by the analysis of polymer properties and monomer conversions. Results suggested that 130 ºC is the process limit, because this temperature provided a nonlinear evolution of number-average molecular weight, i. e., there was a lose of the polymerization control. The results also indicate that for this system there is an optimum temperature of 100 ºC, which provides a relative fast polymerization with a good arquitecture control. Moreover, the kinetic modeling proposed in this present work can be use to analyse every ATRP process, since it is general, and the user needs only to insert the reaction conditions plus the kinetic paramenters available in literature for several monomers and initiators.

6. References

1. Zhao, M., Zhang, H., Ma, F., Zhang, Y., Guo, X., & Zhang, H. (2013). Efficient synthesis of monodisperse, highly crosslinked, and "living" functional polymer microspheres by the ambient temperature iniferter-induced "living" radical precipitation polymerization. *Journal of Polymer Science. Part A, Polymer Chemistry*, *51*(9), 1983-1998. http://dx.doi.org/10.1002/pola.26579.
2. Lessard, B. H., & Marić, M. (2013). Water-soluble/dispersible carbazole-containing random and block copolymers by nitroxide-mediated radical polymerisation. *Canadian Journal of Chemical Engineering*, *91*(4), 618-629. http://dx.doi.org/10.1002/cjce.21676.
3. Porras, C. T., D'Hooge, D. R., Van Steenberge, P. H. M., Reyniers, M. F., & Marin, G. B. (2013). A theoretical exploration of the potential of ICAR ATRP for one- and two-pot synthesis of well-defined diblock copolymers. *Macromolecular Reaction Engineering*, *7*(7), 311-326. http://dx.doi.org/10.1002/mren.201200085.

4. Zhou, Y. N., Li, J. J., & Luo, Z. H. (2012). Synthesis of gradient copolymers with simultaneously tailor-made chain composition distribution and glass transition temperature by semibatch ATRP: from modeling to application. *Journal of Polymer Science. Part A, Polymer Chemistry*, *50*(15), 3052-3066. http://dx.doi.org/10.1002/pola.26091.
5. Goldmann, A. S., Glassner, M., Inglis, A. J., & Barner-Kowollik, C. (2013). Post-functionalization of polymers via orthogonal ligation chemistry. *Macromolecular Rapid Communications*, *34*(10), 810-849. PMid:23625725. http://dx.doi.org/10.1002/marc.201300017.
6. Salian, V. D., & Byrne, M. E. (2013). Living radical polymerization and molecular imprinting: improving polymer morphology in imprinted polymers. *Macromolecular Materials and Engineering*, *298*(4), 379-390. http://dx.doi.org/10.1002/mame.201200191.
7. Yamago, S., Yamada, T., Togai, M., Ukai, Y., Kayahara, E., & Pan, N. (2009). Synthesis of structurally well-defined telechelic polymers by organostibine-mediated living radical polymerization: in situ generation of functionalized chain-transfer agents and selective omega-end-group transformations. *Chemistry*, *15*(4), 1018-1029. PMid:19086048. http://dx.doi.org/10.1002/chem.200801754.
8. Hardy, C. G., Ren, L., Zhang, J., & Tang, C. (2012). Side-chain metallocene-containing polymers by living and controlled polymerizations. *Israel Journal of Chemistry*, *52*(3-4), 230-245. http://dx.doi.org/10.1002/ijch.201100110.
9. Badri, A., Whittaker, M. R., & Zetterlund, P. B. (2012). Modification of graphene/graphene oxide with polymer brushes using controlled/living radical polymerization. *Journal of Polymer Science. Part A, Polymer Chemistry*, *50*(15), 2981-2992. http://dx.doi.org/10.1002/pola.26094.
10. Matyjaszewski, K. (2012). Atom transfer radical polymerization: from mechanisms to applications. *Israel Journal of Chemistry*, *52*(3-4), 206-220. http://dx.doi.org/10.1002/ijch.201100101.
11. Matyjaszewski, K. (2012). Atom Transfer Radical Polymerization (ATRP): current status and future perspectives. *Macromolecules*, *45*(10), 4015-4039. http://dx.doi.org/10.1021/ma3001719.
12. Vieira, R. P., & Lona, L. M. F. (2016). Optimization of reaction conditions in functionalized polystyrene synthesis via ATRP by simulations and factorial design. *Polymer Bulletin*, *73*(7), 1795-1810. http://dx.doi.org/10.1007/s00289-015-1577-z.
13. Zhu, S. (1999). Modeling of molecular weight development in atom transfer radical polymerization. *Macromolecular Theory and Simulations*, *8*(1), 29-37. http://dx.doi.org/10.1002/(SICI)1521-3919(19990101)8:1<29::AID-MATS29>3.0.CO;2-7.
14. D'hooge, D. R., Reyniers, M. F., & Marin, G. B. (2009). Methodology for Kinetic Modeling of Atom Transfer Radical Polymerization. *Macromolecular Reaction Engineering*, *3*(4), 185-209. http://dx.doi.org/10.1002/mren.200800051.
15. Shipp, D. A., & Matyjaszewski, K. (1999). Kinetic analysis of controlled/"living" radical polymerizations by simulations. 1. The importance of diffusion-controlled reactions. *Macromolecules*, *32*(9), 2948-2955. http://dx.doi.org/10.1021/ma9819135.
16. Al-harthi, M., Cheng, L. S., Soares, J. B. P., & Simon, L. C. (2007). Atom-transfer radical polymerization of styrene with bifunctional and monofunctional initiators: experimental and mathematical modeling results. *Journal of Polymer Science*, *45*, 2212-2224. http://dx.doi.org/10.1002/pola.
17. Bentein, L., D'hooge, D. R., Reyniers, M. F., & Marin, G. B. (2011). Kinetic modeling as a tool to understand and improve the nitroxide mediated polymerization of styrene. *Macromolecular Theory and Simulations*, *20*(4), 238-265. http://dx.doi.org/10.1002/mats.201000081.
18. Ray, W. H. (1972). On the mathematical modeling of polymerization reactors. *Journal of Macromolecular Science, Part C: Polymer Reviews*, *8*(1), 1-56. http://dx.doi.org/10.1080/15321797208068168.
19. Vieira, R. P., Ossig, A., Perez, J. M., Grassi, V. G., Petzhold, C. L., Costa, J. M., & Lona, L. M. F. (2013). Simulation of the equilibrium constant effect on the kinetics and average properties of polystyrene obtained by ATRP. *Journal of the Brazilian Chemical Society*, *24*(12), 2008-2014. http://dx.doi.org/10.5935/0103-5053.20130251.
20. Vieira, R. P., Ossig, A., Perez, J. M., Grassi, V. G., Petzhold, C. L., Peres, A. C., Costa, J. M., & Lona, L. M. F. (2015). Styrene ATRP using the new initiator 2,2,2-tribromoethanol: experimental and simulation approach. *Polymer Engineering and Science*, *55*(10), 2270-2276. http://dx.doi.org/10.1002/pen.24113.
21. Vieira, R. P., & Lona, L. M. F. (2016). Kinetic modeling of atom-transfer radical polymerization: inclusion of break reactions in the mechanism. *Polymer Bulletin*, *73*(8), 2105-2119. http://dx.doi.org/10.1007/s00289-015-1596-9.
22. Hindmarsh, A. C. (1983). ODEPACK, a systematized collection of ODE solvers. *Scientific Computing*, *1*, 55-64. Retrieved in 9 November 2015, from https://computation.llnl.gov/casc/nsde/pubs/u88007.pdf
23. Zapata-González, I., Saldívar-Guerra, E., Flores-Tlacuahuac, A., Vivaldo-Lima, E., & Ortiz-Cisneros, J. (2012). Efficient numerical integration of stiff differential equations in polymerisation reaction engineering: computational aspects and applications. *Canadian Journal of Chemical Engineering*, *90*(4), 804-823. http://dx.doi.org/10.1002/cjce.21656.
24. Vieira, R. P., Mokochinski, J. B., & Sawaya, A. C. H. F. (2015). Mathematical modeling of the ascorbic acid thermal degradation in orange juice during industrial pasteurizations. *Journal of Food Process Engineering*, n/a. http://dx.doi.org/10.1111/jfpe.12260.
25. Fu, Y., Mirzaei, A., Cunningham, M. F., & Hutchinson, R. A. (2017). Atom-transfer radical batch and semibatch polymerization of styrene. *Macromolecular Reaction Engineering*, *1*(4), 425-439. http://dx.doi.org/10.1002/mren.200700010.
26. Belincanta-Ximenes, J., Mesa, P. V. R., Lona, L. M. F., Vivaldo-Lima, E., McManus, N. T., & Penlidis, A. (2007). Simulation of styrene polymerization by monomolecular and bimolecular nitroxide-mediated radical processes over a range of reaction conditions. *Macromolecular Theory and Simulations*, *16*(2), 194-208. http://dx.doi.org/10.1002/mats.200600063.
27. Seeliger, F., & Matyjaszewski, K. (2009). Temperature effect on activation rate constants in ATRP: new mechanistic insights into the activation process. *Macromolecules*, *42*(16), 6050-6055. http://dx.doi.org/10.1021/ma9010507.
28. Matyjaszewski, K., Paik, H., Zhou, P., & Diamanti, S. J. (2001). Determination of activation and deactivation rate constants of model compounds in atom transfer radical polymerization 1. *Macromolecules*, *34*(15), 5125-5131. http://dx.doi.org/10.1021/ma010185+.
29. Hui, A. W., & Hamielec, A. E. (1972). Thermal polymerization of styrene at high conversions and temperatures. an experimental study. *Journal of Applied Polymer Science*, *16*(3), 749-769. http://dx.doi.org/10.1002/app.1972.070160319.
30. Fischer, H., & Paul, H. (1987). Rate constants for some prototype radical reactions in liquids by kinetic electron spin resonance. *Accounts of Chemical Research*, *20*(5), 200-206. http://dx.doi.org/10.1021/ar00137a007.

Received: Nov. 09, 2015
Revised: Mar. 11, 2016
Accepted: Mar. 21, 2016